DEMENTIA DISEASE THERAPIES USING EMF ANTENNA EXPOSURE ON A MULTILAYER HUMAN HEAD SIMULATION

Mr. Harshal Ratan Shelar[1], Dr. Nitin S. Patil[2], Mr. Rakesh Kumar Jha[3]

Article History: Received: 12.12.2022 **Revised:** 29.01.2023 **Accepted:** 15.03.2023

Abstract

In this study, we extend previous biological research that shown that repeated electromagnetic field stimulation (REMFS) reduced levels of toxic amyloid-beta (A), which is thought to be the root cause of Alzheimer's disease (AD). In primary human neural cultures, the REMFS values for these exposures were a frequency of 64 MHz and a Specific absorption rate (SAR) of 0.4 to 0.9 W/Kg. The high-frequency simulation system (HFSS/EMPro) software was used in this study to simulate an electromagnetic field (EMF) model. In order to reduce the harmful A levels in our biological investigations in a model of a human skull, we set out to obtain the EM parameters (EMF Frequency and SAR). The simulations carried out here may successfully guide the creation of an exposure system to treat Alzheimer's sufferers. The study took into account a well-known VFH (very high frequency) patch microstrip antenna technology. The decision was made based on the construction's ease of use and suitability for VHF applications. Using a model of a human head, the evaluation of the SAR and temperature distribution on the several head layers—including the skin, fat, dura, cerebrospinal fluid (CSF), grey matter, and brain tissues—was done to determine the effectiveness of the SAR and the safety of temperature rise. Maximum SAR of 0.6 W/Kg was attained using a current pulse of 1 A peak current delivered to the antenna feeder. The layers of the simulated human skull were found to have a range of 0.4 to 0.6 SAR. The antenna's first design suggested a dimension of around 1 m in length and breadth, indicating a stationary useful model for AD treatment. Future directions are provided for exposure systems and wearable antennas that are very effective and comfortable for patients.

Keywords: Dementia, Brain Tissues, Antenna, Simulation

[1]Assistant Professor, Department of Electrical and Electronics Engineering, School of Engineering and Technology, Sandip University, Nashik, Maharashtra 422213
[2]Assistant Professor, Department of Electrical Engineering, Sandip Institute of Technology & Research Centre, Nashik, Maharashtra 422213
[3]Assistant Professor, Department of Electrical Engineering, Sandip Institute of Engineering and Management, Nashik, Maharashtra 422213

Email: [1]harshal.shelar@sandipuniversity.edu.in, [2]nitin.patil@sitrc.org, [3]rakesh.jha@siem.org.in

DOI: 10.31838/ecb/2023.12.s3.137

1. Initialization

Worldwide, Alzheimer's disease (AD) had been on the rise, despite little progress in therapies. Alzheimer's disease (AD) and associated dementias are projected to affect 46 million individuals globally as of 2015, with a predicted prevalence of 131 million by 2050 (Grabher, 2018). The global economy and the healthcare system may be affected by research attempts to slow down or stop the illness. AD is a complicated and varied condition. The medications that the U.S. Food and Drug Administration (FDA) has licenced for the treatment of AD do not halt the disease's development (Bernstein Sideman et al., 2022). Research efforts have also looked at various therapy methods and A antibody therapeutic options to decrease the progression of the illness (Mendiola-Precoma et al., 2016). Considering the unfavourable side effects of medications used to treat AD, there is increased interest in researching alternative, noninvasive processes, such as exposure to electromagnetic fields (EMFs). A recent clinical experiment that exposed AD patients to electromagnetic radiation (915 MHz) reported no physiologic alterations or adverse side effects(Cummings, 2021). Many pilot investigations and short clinical trials have emphasised the potential for neuroenhancement and improvement in cognitive function in healthy persons by noninvasive brain stimulation (NBS), which is currently being investigated as a possible treatment for AD (Kury et al., 2017). The questions of mechanism of action, effectiveness, and repeatability (Kim et al., 2019) needed to be further explored in subsequent studies. The EMF clinical experiment stated above, which employed a high frequency of 915 MHz, is probably ineffective because the radiation does not penetrate to the deep tissues that are crucial for human brain function (only 3 to 4 cm tissue penetration depth). We investigate the use of repetitive electromagnetic field stimulation (REFMS) in this study as a non-invasive possible method to reduce the A-peptide burden seen in AD. The biological effects of REMFS are produced via a non-thermal process that takes place at the molecular level and includes multitarget interactions between signalling pathways (Pistollato et al., 2016). A framework for acceptable human exposure may be established by computer simulations for EMF exposures at a frequency of 64 MHz and a SAR of 0.4–0.9 W/Kg (Weiler et al., n.d.). The creation of portable devices for the treatment of AD is the overall goal of attempts to create noninvasive therapeutic techniques.

In this study, it was discovered that repetitive electromagnetic field stimulation (REMFS), which is thought to be the cause of Alzheimer's disease, was lowering the levels of toxic amyloid-beta (A) (Weiler et al., 2021). (AD). The antenna parameters and the field distribution were obtained using HFSS in response to the preliminary results presented in (Weiler et al., 2021).

The Fieldmark

Maxwell's equations and the heat equations coupled over the different boundaries of the human head tissues yield the following field equations, which are used to calculate the field distribution and the SAR values. The field and SAR distribution throughout the tissues of the human head are provided by the solutions of the following equations using HFFS/EMPro.

$$\nabla \times \mathrm{E} = \mathrm{j}\omega\mu\mathrm{H} \ (1)$$

$$\nabla \times \mathrm{H} = -\mathrm{j}\omega\varepsilon\mathrm{E} \ (2)$$

$$\nabla \cdot \mathrm{E} = 0 \ (3)$$

$$\nabla \cdot \mathrm{H} = 0 \ (4)$$

where is the radian frequency, is the mobility, is the permittivity of the material, and E, H, and are the electric and magnetic fields, respectively.

The power equation for the lossy medium is provided as (Perez et al., 2022), taking into account the conductivity:

$$\mathrm{P_v} = 2\pi f\varepsilon_0\varepsilon''\mathrm{E}^2 \ (5)$$

In lossy medium, the average power is a function of the electric field, E, as shown by:

$$\mathrm{P_{av}} = \int 0.5\sigma|\mathrm{E}^2| \, dv \ (6)$$

dv stands for differential volume.

Electric conductivity causes a material's dielectric loss, which is calculated as follows:

$$\varepsilon'' = \sigma/2\pi\,\varepsilon_0 f \ (7)$$

In the Fourier heat transfer equation (Perez et al., 2019), the microwave dissipated power term is regarded as the source term:

$$\rho C_p \ \partial T/\partial t = k\nabla^2 T + P_v\,(x, y, z, t) \ (8)$$

where Cp is the specific heat capacity and ρ is the mass density.

The equation: may be used to calculate the SAR.

$$\mathrm{SAR} = (\sigma/2\rho)\mathrm{E}^2 \ (9)$$

The following equations provide the thermal energy/temperature change:

$$q = mC_p\nabla T \ (10)$$

The SAR is then can be calculated by $\Delta\mathrm{SAR} = C_p\Delta T/\Delta t$, where ΔT is the change in temperature related to change in SAR by a value of ΔSAR over time Δt.

Antenna architecture

The patch antenna's dimensions are indicated as being in the range of $1.07\mathrm{m} \times 1.38\mathrm{m}$ based on the radiation pattern at 64 MHz. The following equations form the foundation of the Matlab estimation:

The patch's width, w, is determined by(Perez et al., 2019):

$$W = \frac{v_0}{2f_r}\sqrt{\frac{2}{\varepsilon_{reff}+1}} \qquad (11)$$

where v_0 = speed of light, and f_r is the desired frequency. The effective dielectric constant is given by (Mendiola-Precoma et al., 2016; Pistollato et al., 2016):

$$\varepsilon_{r,eff} = \frac{\varepsilon_r + 1}{2} + \frac{\varepsilon_r - 1}{2}\left(1 + 12\frac{h}{W}\right)^{-0.5} \quad (12)$$

where ε_r = dielectric constant of the substrate; $\varepsilon_{r\,eff}$, = effective dielectric constant: $1<\varepsilon_{r\,eff}, < \varepsilon_r$.

The extension length, ΔL, is given by:

$$\Delta L = 0.412h\frac{\left(\varepsilon_{r,eff} + 0.3\right)\left(\frac{W}{h} + 0.264\right)}{\left(\varepsilon_{r,eff} - 0.258\right)\left(\frac{W}{h} + 0.8\right)} \quad (13)$$

where h = height of the dielectric substrate.

3. Result of simulation

The E field, the antenna SAR distribution with and without brain tissues, the scattering S11 parameter, and the SAR at the different levels of the simulated human head were all estimated using HFSS/EMPro. In the brain simulation, the antenna device was modelled for a 64 MHz homogenous pattern and 0.6 SAR. The patch antenna construction is shown in Figure 1. Figures 2 and 3 show the scattering S11 parameter and the current pulse that fed the antenna, respectively.

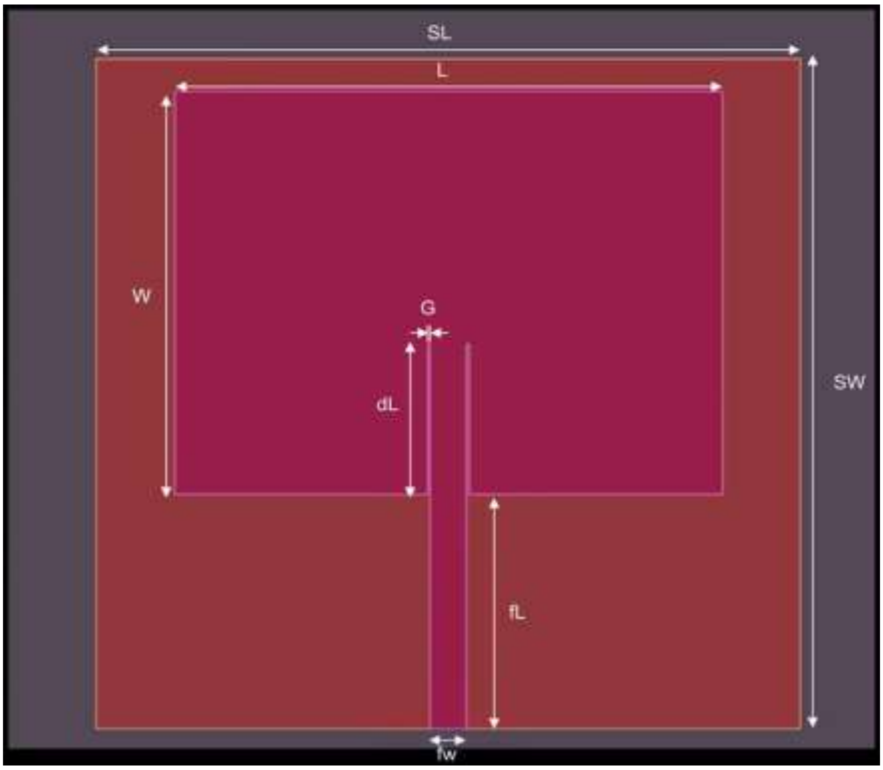

L	1.083 m	g	0.007 m
w	1.4 m	dl	0.403 m
sl	1.8 m	fl	0.603 m
sw	1.8 m	fw	0.092 m

Figure 1: The patch antenna structure

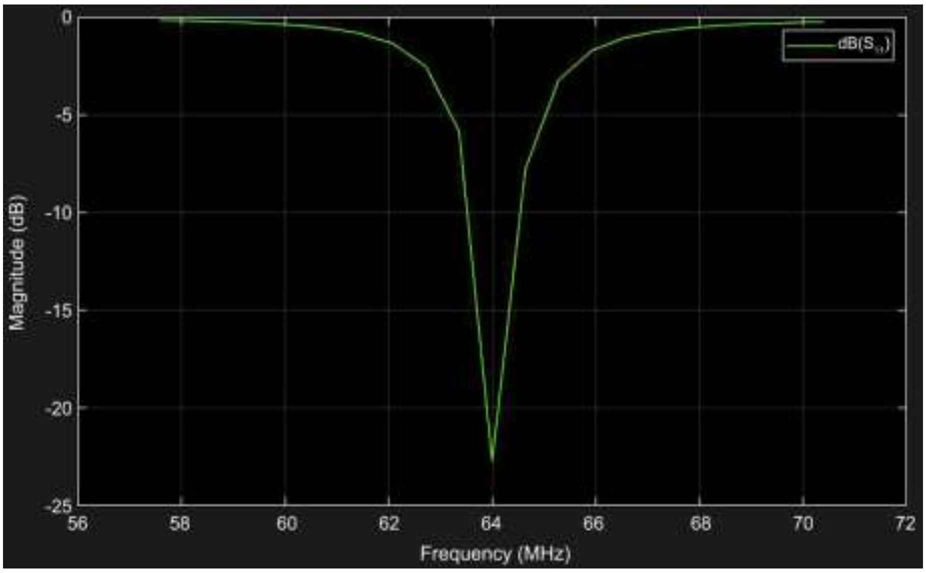

Figure 2: S11 parameter exhibiting 20 dbs magnitude radiation at 64 MHZ

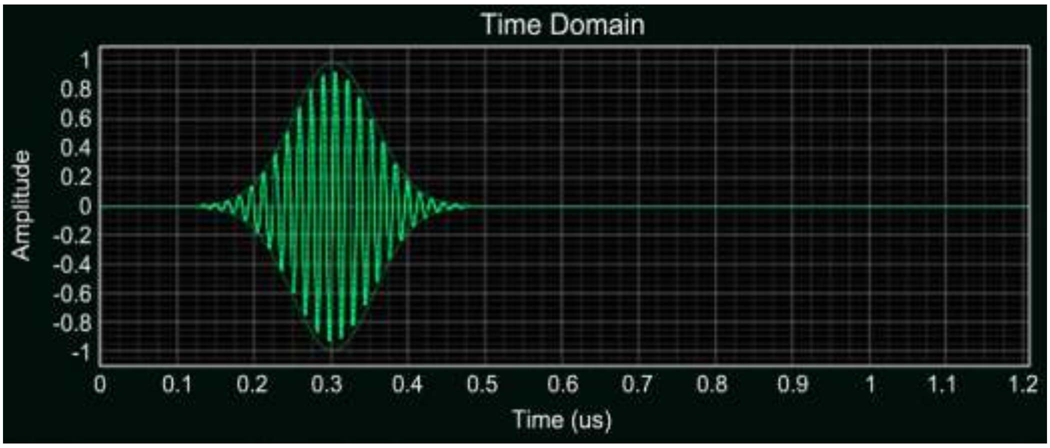

Figure 3: The antenna feed was pulsed with current to provide the necessary 0.6 SAR.

In Figure 4, the antenna E-field is shown. reaching the simulated brain with the largest field provided in the x-direction. Figures 5(a) and 5(b) show the SAR distribution in the XY plane and the XZ plane, respectively. As can be shown, the SAR in the artificial brain tissue spans from 0.2 to 0.9. When the power radiated by the brain tissue outward towards the skin dropped, the SAR value fell. Before the human skull absorbed the power, the SAR value was greater. Figure 6 demonstrates that before a simulated human head absorbs the EMF energy, the simulated antenna produces SAR values that vary from 2 to 9 W/kg.

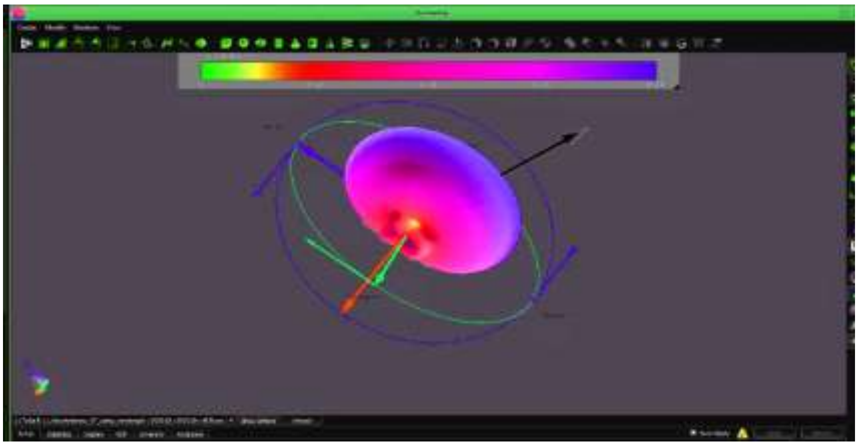

Figure 4: The distribution of the E field from the feed area at x = 0 to Emax at 8.5 V/m

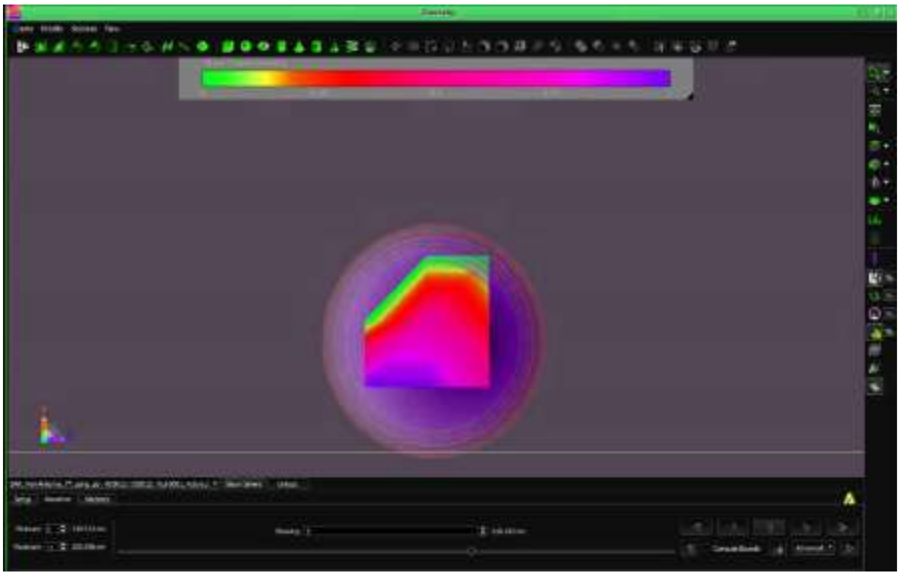

(a)

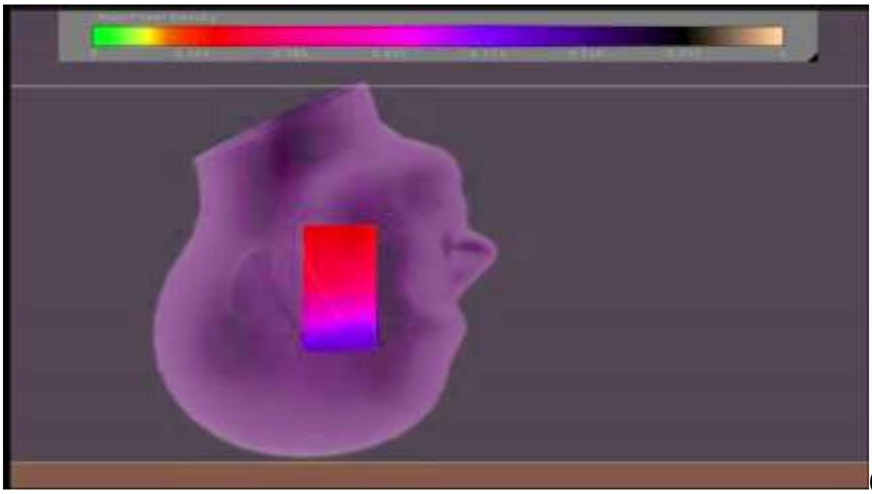

(b)

Figure 5: The SAR distribution in the XY plane and the XZ plane, respectively. 0.2 to 0.9 SAR values are found within tissues.

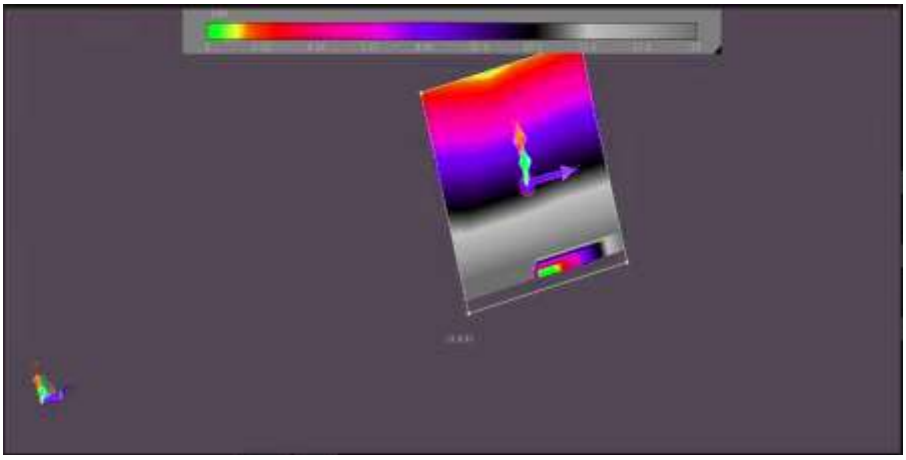

Figure 6: The SAR value that the antenna produced before being applied to the synthetic brain tissue

The 64 MHZ radiating frequency was suitable for the penetration depth required to reach the brain tissue's many layers. The current required to drive the antenna and provide the necessary power is manageable with sufficient penetration depth. It is evident that the input power is adequate to provide the needed SAR. Since that it is the same frequency as MRI imaging, the 64 HMz is also suitable for medical purposes. The findings from the large patch antenna point to a stationary useful model for the EMP device's therapy of Alzheimer's. To maximise the power transfer into the head phantom, the matching impedance between the feeder and antenna needs to be taken into account.

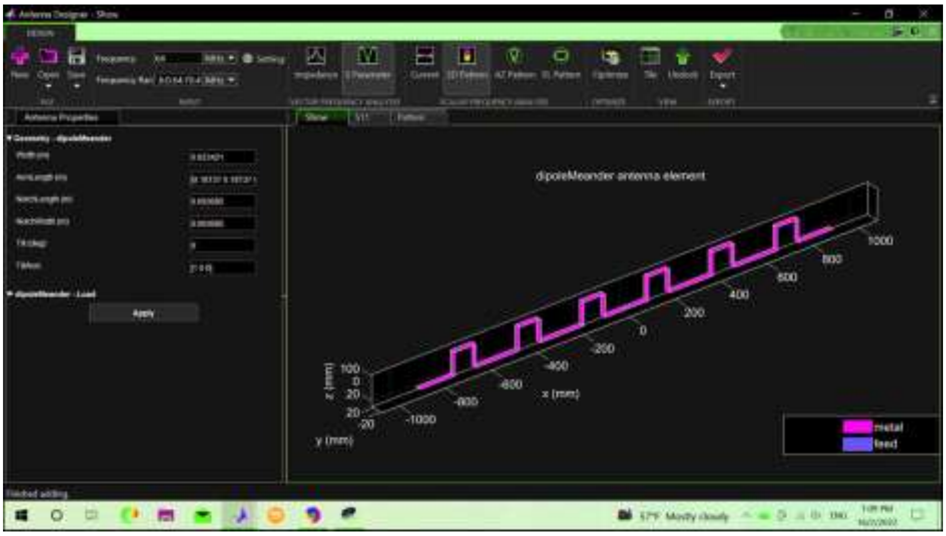

(a) The antenna structure

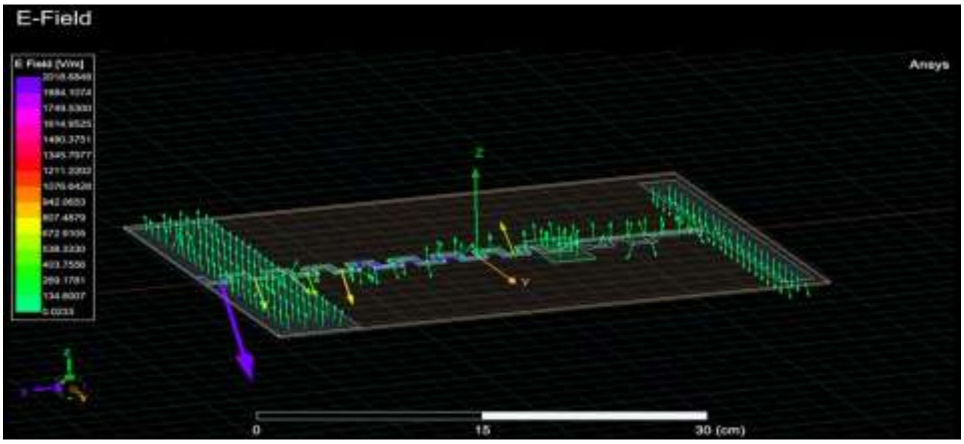

(b) The E field distribution

Figure 7: Future suggested antenna, (a) antenna construction, and (b) field dispersion for wearable device system

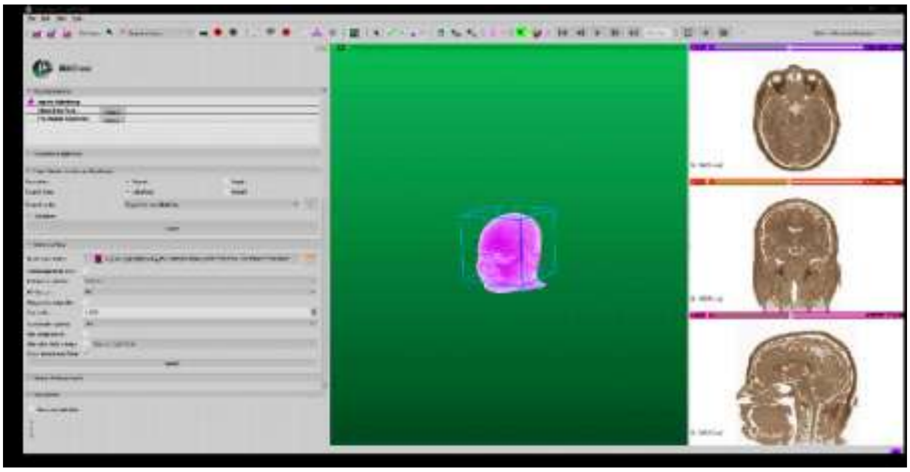

Figure 8: Detailed anatomical layers in the proposed head phantom simulation for improving SAR results

3. Conclusion and Future Scope

In this study, we employed a straightforward strip antenna and HFSS to estimate the SAR values for various human head tissues. The antenna's size, which was discovered to be in the metres range, points to the usage of a stationary EMR system for AD treatment. For the purpose of creating a manageable wearable device system that is comfortable to wear, a meander line antenna may be a suitable choice. A suggested antenna for a wearable device system is shown in Figure 7 in helmet form. The system was originally simulated, and Figure 7 shows the field distribution (b). This antenna wearable system's specifics will be decided upon later.

Wearable antenna design requires a precise human model. The Zubal anthropomorphic phantom, where real X-ray CT scans were recreated, may improve the simulation's fidelity. The head phantom under consideration for future development is shown in Figure 8. Moreover, anthropomorphic phantom voxel data from Digital Imaging and Communication in Medicine (DICOM) may be used to improve the simulation's accuracy for specific patients.

4. Reference

Bernstein Sideman, A., Al-Rousan, T., Tsoy, E., Piña Escudero, S. D., Pintado-Caipa, M., Kanjanapong, S., Mbakile-Mahlanza, L., Okada de Oliveira, M., la Cruz-Puebla, D., & Zygouris, S. (2022). Facilitators and Barriers to Dementia Assessment and Diagnosis: Perspectives From Dementia Experts Within a Global Health Context. Frontiers in Neurology, 232.

Cummings, J. (2021). New approaches to symptomatic treatments for Alzheimer's disease. Molecular Neurodegeneration, 16(1), 1–13.

Grabher, B. J. (2018). Alzheimer's Disease and the Effects it has on the Patient and their Family. Journal of Nuclear Medicine Technology.

Kim, T. D., Hong, G., Kim, J., & Yoon, S. (2019). Cognitive enhancement in neurological and psychiatric disorders using transcranial magnetic stimulation (TMS): a review of modalities, potential mechanisms and future implications. Experimental Neurobiology, 28(1), 1–16.

Kury, F. S. P., Baik, S. H., & McDonald, C. J. (2017). Cardioprotective Drugs and Incident Dementias in Medicare's Big Data. AMIA.

Mendiola-Precoma, J., Berumen, L. C., Padilla, K., & Garcia-Alcocer, G. (2016). Therapies for prevention and treatment of Alzheimer's disease. BioMed Research International, 2016.

Perez, F. P., Rahmani, M., Emberson, J., Weber, M., Morisaki, J., Amran, F., Bakri, S., Halim, A., Dsouza, A., & Yusuff, N. M. (2022). EMF Antenna Exposure on a Multilayer Human Head Simulation for Alzheimer Disease Treatments. Journal of Biomedical Science and Engineering, 15(5), 129–139.

Perez, F. P., Rizkalla, J., Jeffers, M., Salama, P., Chumbiauca, C. N. P., & Rizkalla, M. (2019). The Effect of Repeated Electromagnetic Fields Stimulation in Biological Systems. In Ionizing and Non-ionizing Radiation. IntechOpen.

Pistollato, F., Ohayon, E. L., Lam, A., Langley, G. R., Novak, T. J., Pamies, D., Perry, G., Trushina, E., Williams, R. S. B., & Roher, A. E. (2016). Alzheimer disease research in the 21st century: past and current failures, new perspectives and funding priorities. Oncotarget, 7(26), 38999.

Weiler, M., Moreno-Castilla, P., Starnes, H. M., Melendez, E. L. R., Stieger, K. C., Long, J. M., & Rapp, P. R. (2021). Effects of repetitive Transcranial Magnetic Stimulation in aged rats depend on pre-treatment cognitive status: Toward individualized intervention for successful cognitive aging. Brain Stimulation, 14(5), 1219–1225.

Weiler, M., Stieger, K. C., Long, J. M., & Rapp, P. R. (n.d.). Transcranial magnetic stimulation in Alzheimer's disease: Are we ready? eNeuro 2020, 7. ENEURO.